

Published in final edited form as:

J Agric Food Chem. 2013 September 25; 61(38): . doi:10.1021/jf4023004.

Nanoencapsulation Enhances Epigallocatechin-3-Gallate Stability and Its Anti-atherogenic Bioactivities in Macrophages

Jia Zhang[#], Shufang Nie[#], and Shu Wang^{*}

Nutritional Science Program, Texas Tech University, Lubbock, TX, 79409

[#] These authors contributed equally to this work.

Abstract

We have successfully synthesized (–)-epigallocatechin-3-gallate (EGCG) encapsulated nanostructured lipid carriers (NLCE) and chitosan coated NLCE (CSNLCE) using natural lipids, surfactant, chitosan and EGCG. Nanoencapsulation dramatically improved EGCG stability. CSNLCE significantly increased EGCG content in THP-1 derived macrophages compared with nonencapsulated EGCG. As compared to 10 μ M of nonencapsulated EGCG, both NLCE and CSNLCE at the same concentration significantly decreased macrophage cholesteryl ester content. NLCE and CSNLCE significantly decreased mRNA levels and protein secretion of monocyte chemoattractant protein-1 (MCP-1) levels in macrophages, respectively. These data suggest that nanoencapsulated EGCG may have a potential to inhibit atherosclerotic lesion development through decreasing macrophage cholesterol content and MCP-1 expression.

Keywords

EGCG; nanostructured lipid carriers; atherosclerosis; macrophage; stability; uptake

INTRODUCTION

Green tea is made from the dried leaves of the *Camellia sinensis* plant and has been considered a healthy beverage since ancient times. Different from fermented black tea and partially fermented oolong tea, green tea is produced from direct drying of fresh green tea leaves by hot steam and air. During this process, polyphenol oxidase is inactivated and catechins are preserved¹. Green tea contains more catechins than black or oolong tea². Catechins constitute about 14 to 33% of the dry green tea leaf weight^{1,3}. (–)-Epigallocatechin-3-gallate (EGCG) is the most abundant green tea catechin and comprises 25 to 55% of the total catechins^{1,3}. Over the past few decades many scientific and medical studies have already demonstrated many health benefits of green tea including anti-atherogenic, anti-inflammatory and anti-tumorigenic properties⁴.

Cardiovascular disease (CVD) refers to the class of diseases that involve the heart and blood vessels. CVD is the leading cause of death in the United States and worldwide^{5,6}. About half of the CVD death is caused by atherosclerosis, which is a progressive disease characterized by lipid plaque formation in arteries, resulting in insufficient blood supply to heart muscle, brain or peripheral tissues (for example legs). Increased lipid accumulation and inflammatory responses are the major causes of atherosclerosis^{7,8}. Monocyte chemoattractant protein 1 (MCP-1) promotes the recruitment of monocytes into the aortic

^{*} Address requests for reprints and correspondence to Shu Wang, Nutritional Science Program, Texas Tech University, Box 41240, Lubbock, TX 79409-1240 shu.wang@ttu.edu (S. Wang) Phone: (806) 742-3068, extension 282 Fax: (806) 742-3042.

intima layer⁷. Upon the migration, monocytes are differentiated into macrophages in response to macrophage colony-stimulating factor. These macrophages express scavenger receptors, which increase the uptake of minimally modified low density lipoprotein (LDL), especially minimally oxidized LDL (oxLDL)⁹. After macrophages accumulate cholesterol, they are transformed into foam cells. Foam cells can secrete many inflammatory factors including MCP-1, which further recruit more monocytes, resulting in increased number of macrophages and later foam cells in the artery wall. After foam cells die, lipids (primarily cholesterol) are accumulated on the artery wall and atherosclerotic plaque is formed. Total cholesterol (TC) in macrophages includes cholesteryl ester (CE), a storage form of cholesterol, and free cholesterol (FC), which can be transported out of macrophages via a process termed reverse cholesterol transport. Foam cells formation and cholesterol accumulation in the vessel intima characterize the atherosclerotic lesion⁹. Therefore, macrophages play an important role in atherosclerotic lesion progression by facilitating cholesterol accumulation and increasing inflammatory responses in aortic walls.

EGCG has a potential to decrease the release of inflammatory factors and reduce cholesterol accumulation in macrophages¹⁰⁻¹³, which may in turn prevent atherosclerotic lesion development. When apolipoprotein E null mice are treated with daily intraperitoneal injections of EGCG at a dose of 10 mg/kg body weight, cuff-induced evolving atherosclerotic lesion size is reduced by 55% after 21 days treatment¹⁴. Human studies indicate that EGCG can maintain cardiovascular health, but the evidence is inconclusive regarding the effectiveness for CVD prevention or treatment^{15, 16}. The major problems are its low stability and bioavailability in humans or research animals¹⁷⁻¹⁹. The oral bioavailability of EGCG after drinking tea containing catechins at 10 mg/kg body weight is about 0.1% in humans and research animals^{18, 20}. The peak plasma EGCG concentration is 0.15 μ M after drinking 2 cups of green tea¹⁹. Moreover, EGCG is unstable in water and physiological fluid *in vitro*²¹. EGCG stability is lowered by various metabolic transformations including methylation, glucuronidation, sulfation and oxidative degradation^{22, 23}. Hence, there is a critical need to use biocompatible and biodegradable carriers to increase EGCG stability and uptake.

Nanotechnology involves the control of matter, generally in the range of 100 nm or smaller²⁴. Nanocarriers may increase bioavailability of encapsulated EGCG, enhance its stability, lower its toxicity through preventing EGCG from prematurely interacting with the biological environment and improve intracellular penetration. Even though nanoparticles have many beneficial effects, they also have many disadvantages including expensive cost, complex synthesis procedures and potential side-effects. We successfully produced biocompatible and biodegradable EGCG encapsulated nanostructured lipid carriers (NLCE), which are composed of natural lipids, surfactant, EGCG and water. Nanostructured lipid carriers (NLCs) have received considerable attention because of their small size, stability, biocompatibility and biodegradability, low cytotoxicity, and easily scaled-up synthesis processes²⁵. The NLC structure is composed of a hydrophilic shell and a hydrophobic lipid core, which is solid at room temperature. Chitosan, a natural polysaccharide, is an absorption enhancer^{26, 27}. We have synthesized chitosan-coated NLCE (CSNLCE). Our hypothesis is that NLCs and CSNLCEs can increase EGCG stability, increase EGCG uptake by THP-1 derived macrophages, and decrease cellular CE content and lower expression and secretion of inflammatory factors in those macrophages.

MATERIALS AND METHODS

Chemicals and reagents

EGCG (>95%), glyceryl tridecanoate, glyceryl tripalmitate, chitosan with medium molecular weight of 190,000–310,000, phorbol 12-myristate 13-acetate (PMA), *Escherichia*

coli lipopolysaccharide were purchased from Sigma-Aldrich Chemical Co. (St. Louis, MO). Kolliphor HS15 was given as gift from BASF Chemical Co., USA (Florham Park, NJ). Soy lecithin (>95%) and 7-nitro-2-1, 3-benzoxadiazol-4-yl-phosphatidylcholine (NBD-PC) were purchased from Avanti Polar Lipids (Alabaster, AL). Trizol reagent, SuperScript™ III reverse transcriptase and power SYBR green master mix were purchased from Life Technologies Co. (Carlsbad, CA).

Preparation of NLCE and CSNLCE

NLC was prepared from a lipid mixture composed of the following lipids in wt%: 9.3% soy lecithin, 40.0% glyceryl tridecanoate, 6.7% glyceryl tripalmitate, 44.0% Kolliphor HS15 (polyoxyethylated 12-hydroxystearic acid, a non-ionic surfactant), and an aqueous mixture containing 2.6% EGCG and 1% of NaCl in deionized water. A novel phase inversion-based process was used in preparing NLCE²⁸. Briefly, oil and aqueous phase were heated to 85°C and mixed together. Then, the mixture was treated with three temperature cycles from 60 to 85°C and from 85 to 60°C at a rate of 4°C per min and stirred at 375 rpm per min on a magnetic stirrer. In the last cycle, when the mixture was cooled to 70°C, cold deionized water (0°C) was added to the mixture. The volume ratio of cold water to lipid was 35:1 in this study. The fast cooling-dilution process resulted in NLCE formation. Afterward, a slow magnetic stirring was applied to the suspension for 45 min. Void nanostructured lipid carriers (VNLC) were synthesized by using the same method without adding EGCG. All steps in the preparation of VNLC and NLCE were performed under nitrogen to prevent EGCG and lipid degradation. NLCE and VNLC were concentrated and coated with 6 mg/mL chitosan using a magnetic stirrer for 40 min at 4°C to form CSNLCE and chitosan-coated VNLC (VCSNLC), respectively. The final concentration of chitosan in CSNLCE and VCSNLC was 2 mg/mL.

Encapsulation efficiency and loading capacity determination

The total EGCG concentration (C_{total}) in the nanocarrier solution was measured using a high performance liquid chromatography (HPLC) system (Waters Co., Milford, MA) with a C18 reverse-phase column (150 mm×4.6 mm, 5 μm size) and Waters 2489 UV/Visible detector. The mixture of water/acetonitrile/ethyl acetate/sulfuric acid (86:12:2:0.043, v:v:v:v) was used as a mobile phase with flow rate of 1 mL/min. The detection wavelength was selected as 254 nm. Free EGCG was separated from nanoencapsulated EGCG using an ultrafiltration method (Millipore Amicon Ultra-15) at 10,000 \times g at 4°C for 20 min, and measured by the HPLC system (C_{free}). In order to calculate the loading capacity, a certain volume of NLCE (V) was dried using a vacuum freeze-drying system (FreeZone 4.5 plus, Labconco, Kansas City, MO). The weight of dried NLCE was expressed as W_{NPS} . Dried NLCE was only used for measuring loading capacity. Nanoparticle suspension was used for the rest experiments. The encapsulation efficiency and loading capacity of EGCG in the nanocarriers were calculated according to the following equations, respectively:

$$\text{Encapsulation efficiency} = (C_{\text{total}} - C_{\text{free}}) / C_{\text{total}} \times 100\%$$

$$\text{Loading capacity} = (C_{\text{total}}V - C_{\text{free}}V) / W_{\text{NPS}} \times 100\%$$

Particle size, zeta potential and morphology of nanocarriers

The mean particle size was measured by dynamic light scattering (DLS), polydispersity index (PI) and zeta potential of nanocarriers were measured using a ZetaPALS analyzer (Brookhaven Corporation, Holtsville, NY). The morphology of the NLCE and CSNLCE

was examined using a transmission electron microscope (TEM) instrument (200Kv Hitachi H-8100, Tokyo, Japan).

Stability study of NLCE, CSNLCE and nonencapsulated EGCG

The stability of NLCE, CSNLCE and nonencapsulated EGCG were determined in 1 X phosphate buffered saline (1 X PBS) at pH=1.0, 3.0, 5.0, 7.4. Hydrochloric acid was used to adjust pH. The final concentration of nanoencapsulated and nonencapsulated EGCG was 100 μM . The solutions were stored in tightly closed vials and incubated at 37°C. EGCG concentrations were measured after incubation for 0, 0.25, 0.5, 0.75, 1.0, 1.5, 2.0 and 3.0 hours. To determine the EGCG stability at different temperatures, 100 μM of nonencapsulated EGCG and nanoencapsulated EGCG (NLCE and CSNLCE) dissolved in 1XPBS (pH 7.4, ionic strength 157.5 mM) was incubated at 4°C for 14 days, 22°C for 19 hours and 37°C for 3 hours. We also measured their stability in RPMI1640 cell culture medium at 37°C with or without cells, and with or without superoxide dismutases (SOD, 5U/mL).

In vitro release study

The *in vitro* release behavior of nonencapsulated EGCG and NLCE were measured in 1 X PBS (pH 5.0) using a dialysis method. Samples of 1.0 mg of nonencapsulated EGCG and equivalent amount in NLCE were dissolved in 2 mL of 1 X PBS (pH 5.0) and then placed in the dialysis bags with MWCO 6,000-8,000. The dialysis bags were dipped in a conical flask containing 25 mL of 1 X PBS (pH 5.0) (dissolution medium) at 37°C and stirred at 250 rpm/min. The dissolution medium was totally replaced by fresh pre-warmed medium every two hours in order to minimize the effect of EGCG degradation. The EGCG released into the medium was determined every 30 min using the HPLC system.

Cytotoxicity analysis

Human monocytic THP-1 cell line was purchased from the American Type Tissue Culture Collection (ATCC, Manassas, VA) and cultured in the RPMI1640 medium following to ATCC instructions. THP-1 cells (3×10^4 /well) in a 96-well plate were differentiated into macrophages by incubating with 50 ng/mL PMA for 72 hours. The THP-1 derived macrophages were treated with 1 X PBS, nonencapsulated EGCG, VNLC, NLCE, VCSNLC, CSNLCE dissolved in 1 X PBS (pH 7.4) for 18 hours. Three EGCG concentrations (5 μM , 10 μM and 20 μM) were tested. The cell viability was measured using a 3-(4, 5-dimethylthiazol-2-yl)-2,5-diphenyltetrazolium bromide (MTT) assay as previously described²⁹. Three independent experiments were conducted with six replicates within one experiment.

The binding and uptake of fluorescent dye-labeled nanocarriers

We used the above phase inversion-based process to synthesize NBD-PC-labeled VNLC (NBD-VNLC) by replacing 1.0 mol% of total lipids with NBD-PC, and coated them with chitosan to form NBD-PC-labeled VCSNLC (NBD-VCSNLC). After incubating THP-1 derived macrophages with NBD-VNLC or NBD-VCSNLC, or 1 X PBS (pH 7.4) used as control at 4°C and 37°C, cellular binding and uptake of NBD-VNLC and NBD-VCSNLC were observed under a fluorescence microscopy (Olympus, USA) as previously described²⁹. Microscopy settings were identical for all measures to allow equal comparison of the images. Fluorescence intensities were quantified using the NIH imageJ software.

Cellular EGCG content

THP-1 derived macrophages were incubated with 100 μM of nonencapsulated EGCG and nanoencapsulated EGCG (NLCE and CSNLCE) in RPMI1640 medium with or without

SOD (5U/mL) for 2 and 4 hours at 4°C or 37°C. After washing cells, the cellular EGCG was extracted and determined as previously described²⁹. Total cellular protein levels were determined by using a bicinchoninic acid (BCA) kit (Pierce, Rockford, IL). Cellular EGCG content was expressed as μg of EGCG per mg of protein.

Minimally oxidized LDL preparation and cellular cholesterol content measurement

LDL was isolated from human plasma by a sequential ultracentrifugation method³⁰. Minimally oxidized LDL (oxLDL) was prepared by an adaptation of a previously described method³⁰. THP-1 derived macrophages of $1.5 \times 10^6/\text{well}$ in 6-well plates were incubated with or without 40 mg protein/mL of minimally oxLDL in combination with the following treatments: 1XPBS, nonencapsulated EGCG, VNLC, NLCE, VCSNLC and CSNLCE containing 10 μM of EGCG for 18 hours. After cellular lipid extraction using a chloroform and methanol mixture (2:1, v/v), FC and TC were measured using a HPLC system as previously described³⁰. Stigmasterol was used as internal standard. Delipidated cellular protein levels were determined using a BCA kit. CE was calculated as the difference between TC and FC and expressed as μmol of cholesterol per gram of protein.

Secretion of inflammatory factors

THP-1 derived macrophages were pretreated with 10 μM of VNLC, VCSNLC, NLCE, CSNLCE, EGCG and 1 X PBS for 2 hours. Then, 50 ng/mL of *Escherichia coli* lipopolysaccharide (Sigma, St Louis, MO) was added into each well and incubated for additional 16 hours. Tumor necrosis factor alpha (TNF α), interleukin-6 (IL-6) and MCP-1 protein concentrations in the culture medium were determined using DuoSet ELISA kits (R&D Systems, Minneapolis, MN) as previously described³⁰.

Real-time polymerase chain reaction

RNA was extracted from THP-1 derived macrophages using a Trizol reagent. cDNA was synthesized from RNA using SuperScriptTM III reverse transcriptase according to the manufacturer's instructions. MCP-1 and TNF α primers were designed and tested in our previous publication³⁰. Beta-actin was used as an endogenous control. cDNA levels of MCP-1 and TNF α were measured using power SYBR green master mix on a Real-time PCR system (Eppendorf, Hauppauge, NY). mRNA-fold change was calculated using the $2^{-(\Delta\Delta C(T))}$ method³⁰.

Statistical analysis

Data analysis was conducted using Statistical Package for the Social Sciences (SPSS). One-way ANOVA followed by Tukey HSD Post Hoc test was performed to compare multiple group means. Independent student's *t-test* was performed to compare two group means. Differences were considered statistically significant at $p < 0.05$. Data in figures and tables are expressed as means \pm standard deviation (SD).

Safety information

The MTT dye reagent is hazardous; avoid contact with skin and eyes. MTT solvent is flammable and corrosive. Wear lab coat, gloves and safety glasses when working with this reagent.

RESULTS AND DISCUSSION

Characteristics of nanocarriers

EGCG is a promising natural compound for atherosclerosis prevention and treatment. However, its low levels of stability and cellular bioavailability limit its anti-atherogenic

activity. Two approaches have been used to increase its stability and bioactivities: (i) formation peracetate ester of EGCG³¹ or EGCG-docosapentaenoic acid ester³²; (ii) using nanocarriers such as nanoliposomes²⁹ and NLCs³³. The chemical modification makes lipophilic EGCG prodrugs, which require chemical cleavage before releasing nonencapsulated EGCG. Nanoliposomes *per se* are not stable, and encapsulated compound can be leaked out. NLCs do not have those problems, and have been widely used in pharmaceutical and nutraceutical research. In this study, NLCE and CSNLCE were successfully synthesized using biocompatible and biodegradable triglyceride, phosphatidylcholine, Kolliphor HS15, NaCl, chitosan and EGCG. The size of VNLC and NLCE were about 45 nm in diameter, and coating them with chitosan increased the size to about 50 nm (**Table 1**). PI values were relatively low (<0.3), which indicates a high level of uniformity (**Table 1**). Studies have shown that nanocarriers smaller than 100 nm are cleared much slower than large carriers by the reticulo-endothelial system in the liver and spleen^{24,34}. VNLC and NLCE were negative charged. After coating them with chitosan, VCSNLC and CSNLCE became slightly larger and positively charged (**Table 1**). Chitosan is a natural and biocompatible polysaccharide obtained by deacetylation of chitin from exoskeleton of crustaceans like crabs and shrimps, which can enhance the stability and bioavailability of nanocarriers and nanoencapsulated compounds³⁵.

Table 1 also showed the changes of particle size, PI and zeta potential of NLCE and CSNLCE in deionized water at 4°C and 37°C. After 4°C storage for 50 days, the size, PI and zeta potential of VNLC, NLCE and VCSNLC were slightly changed, but the size and PI of CSNLCE were increased more than 1.3 fold. Surface charge is important in nanocarrier systems. In general, higher absolute surface charge leads to stronger repulsion interactions among nanocarriers, and hence higher stability. After incubation at 37°C for 24 hours, the size and PI of nanocarriers did not change dramatically, but the absolute zeta potential values were decreased. In this study, mixing glyceryl tridecanoate and glyceryl tripalmitate can form less perfect crystals in the lipid core, which can accommodate more EGCG. The encapsulation efficiency is about 99% and loading capacity is around 3%. Glyceryl tridecanoate is solid at room temperature and liquid in body temperature, which can improve EGCG storage stability *in vitro* and bioactivity *in vivo*. Both NLCE and CSNLCE were spherical under a transmission electron microscope (TEM) (**Figure 1A and 1B**). The average size of NLCE and CSNLCE measured using TEM was consistent to the dynamic light scattering measures. Many studies indicated that the nature and amounts of surfactants and lipids determine the characteristics of nanocarriers, such as particle size and encapsulation efficiency^{33,36}. Higher lipid amounts (larger hydrophobic core) can accommodate more EGCG, but form large nanocarriers³⁷. The particle size of nanocarriers was dependent on the ratio of lipids to surfactants. In consistent to other studies^{33,36}, we found that as the ratio of triglycerides to Kolliphor HS15 was decreased, the size of nanocarriers was decreased (data not shown). Based on these preliminary data, we chose 1:1 ratio of triglycerides to Kolliphor HS15, which gave small size (48 nm in diameter) and high encapsulation efficiency (about 99%).

The chemical stability of NLCE, CSNLCE and nonencapsulated EGCG

We measured the chemical stability of 100 μ M of nonencapsulated and nanoencapsulated EGCG in different temperatures and pH values. NLCE, CSNLCE and nonencapsulated EGCG were stable in the acidic pH ranging from 1.0 to 5.0 at 37°C for 3 hours (data not shown). EGCG is unstable under alkaline or neutral conditions³⁸. In the neutral pH 7.4, nanoencapsulation significantly increased the percentage of EGCG remaining at three tested temperatures (4°C, 25°C and 37°C) (**Figure 2**). At 4°C, 100% of nonencapsulated EGCG was degraded after 1 day, whereas the degradation rate of EGCG in NLCE and CSNLCE was less than 5%. After 14 days, 75% and 25% of EGCG were remained in CSNLCE and

NLCE at 4°C (**Figure 2A**). After incubating them for 8 hours at 22°C, the percentage of remained EGCG in nonencapsulated EGCG, NLCE and CSNLCE was 1.5%, 55% and 89%, respectively (**Figure 2B**). At 37°C, nonencapsulated EGCG were completely degraded after 3 hours, however, the percentage of remained EGCG in NLCE and CSNLCE was 33% and 64%, respectively (**Figure 2C**). In addition, concentrated nanoencapsulated EGCG can be stored at 4°C for a long period of time without obvious degradation. After storing NLCE and CSNLCE in neutral 1 X PBS containing 3000 μM of nanoencapsulated EGCG at 4°C for 50 days, we still detected 82% and 92% of EGCG in NLCE and CSNLCE, respectively. These results indicated that nanoencapsulation significantly increased EGCG stability. NLC has a solid lipid core at room temperature. Amphiphilic and pH sensitive compounds can be easily encapsulated into the lipid core and are stable in the solid lipid core³⁹. Recently, many studies indicated that green tea catechins may undergo degradation, oxidation, epimerization and polymerization, which could be contributed by many factors such as temperature, pH of the system, oxygen levels and the presence of metal ions^{3,40}. Nanoencapsulation increases EGCG stability through preventing EGCG from prematurely interacting with the biological environment^{33,35,41}.

Nanoencapsulation also enhances EGCG stability in RPMI1640 medium at 37°C. After incubating 100 μM of nonencapsulated and nanoencapsulated EGCG in RPMI1640 medium without THP-1 derived macrophages for 1 hour, the percentage of remained EGCG in nonencapsulated EGCG, NLCE and CSNLCE was 3.7%, 27% and 31%, respectively (**Figure 3A**). As compared to 1 X PBS, RPMI1640 medium decreased the stability of nonencapsulated and nanoencapsulated EGCG (**Figure 2C and 3A**), which is consistent with EGCG stability order in another study: water > 1XPBS > culture medium⁴². The presence of metal ions and proteins in cell culture might contribute to decreased EGCG stability²¹. SOD dramatically increased nonencapsulated EGCG stability in RPMI1640 medium (**Figure 3B**). Therefore, the stability of NLCE, CSNLCE and nonencapsulated EGCG was similar in the presence of SOD at 37°C (**Figure 3B**). In the neutral 1 X PBS and medium, EGCG is easily auto-oxidized, forming EGCG dimmers. After adding SOD into the incubation medium, auto-oxidation and dimer formation were inhibited^{21,42}.

We measured EGCG concentrations in RPMI1640 medium in the presence of THP-1 derived macrophages, which were treated with 100 μM of NLCE, CSNLCE and nonencapsulated EGCG at 4°C and 37°C. Even though macrophages took up nonencapsulated and nanoencapsulated EGCG from medium, the EGCG concentrations in the medium were higher in the presence of macrophages compared to in the absence of cells at 37°C (**Figure 3A-B and 4C-D**). The concentrations of nanoencapsulated and nonencapsulated EGCG in culture medium were higher at 4°C compared to 37°C (**Figure 4**). SOD increased the concentrations of nanoencapsulated and nonencapsulated EGCG in culture medium at 4°C and 37°C (**Figure 4B and Figure 4D**). Hong J. et al. demonstrated that adding 50 μM of EGCG to cell culture medium increased H₂O₂ production, which can decrease EGCG stability²¹. However, the amount of H₂O₂ was decreased in the presence of cells²¹. Other studies indicated that increased H₂O₂ production by EGCG instead of direct effects of EGCG resulted in cancer cell growth inhibition and apoptosis *in vitro*^{43,44}. Cells in the culture medium can produce glutathione peroxidase and catalase, which can decompose H₂O₂ and further improve EGCG stability^{43,44}. Based on these data, SOD (5U/mL) was used to stabilize EGCG for measuring the uptake of nonencapsulated and nanoencapsulated EGCG by macrophages⁴².

Cellular binding and uptake of NBD-nanocarriers

The binding and uptake of NBD-labeled nanocarriers in THP-1 derived macrophages were observed under a fluorescence microscope after treating macrophages with NBD-VNLC

(**Figure 5A**) and NBD-VCSNLC (**Figure 5B**) for 2, 4, 6, 18 and 24 hours at 37°C and 4 hours at 4°C. The green and blue colors denote NBD-nanocarriers and cell nuclei, respectively. More NBD-nanocarriers were bound and taken up by macrophages at 37°C compared to 4°C. As incubation time was increased, the binding and uptake of NBD-VNLC and NBD-VCSNLC in macrophages were gradually increased and reached the peak at hour 18. After incubation for 24 hours, the binding and uptake of NBD-VNLC and NBD-VCSNLC in macrophages were decreased (**Figure 5C**). Nanocarriers degradation caused by enzymes or environmental factors may partially contribute to the decreased uptake after long-term incubation. As compared to NBD-VNLC, more NBD-VCSNLC was taken up and bound to macrophages (**Figure 5A-C**). The data further confirm chitosan is an uptake enhancer. According to fluorescence imaging data, the binding and uptake of NBD-VNLC and NBD-VCSNLC in macrophages were temperature- and time-dependent (**Figure 5C**).

Macrophage EGCG content

To measure the cellular EGCG content, THP-1 derived macrophages were incubated with 100 μM of nonencapsulated EGCG, NLCE and CSNLCE at 4°C or 37°C for 2 and 4 hours. After incubation at 37°C for 2 hours in the absence of SOD, the EGCG content in macrophages treated by nonencapsulated EGCG, NLCE and CSNLCE was 0.031, 0.096, 0.14 $\mu\text{g}/\text{mg}$ protein, respectively (data not shown). In the presence of SOD, the EGCG content was increased to 0.098, 0.176, 0.307 $\mu\text{g}/\text{mg}$ protein in macrophages treated by nonencapsulated EGCG, NLCE and CSNLCE at 37°C for 2 hours, respectively (**Figure 6**). After incubation at 37°C for 4 hours in the presence of SOD, the EGCG content in macrophages treated by nonencapsulated EGCG, NLCE and CSNLCE was 0.109, 0.458, 0.853 $\mu\text{g}/\text{mg}$ protein, respectively (**Figure 6**). SOD significantly increased cellular EGCG content among all treatments, which might be partially due to its function in enhancing EGCG stability. No matter in the absence or presence of SOD, nanoencapsulated EGCG, especially CSNLCE, dramatically increased macrophage EGCG content compared to nonencapsulated EGCG (**Figure 6**). Increased macrophage EGCG content by NLCE and CSNLCE could be partially caused by enhanced EGCG stability. Except nonencapsulated EGCG, 4-hour incubation resulted in higher macrophage EGCG content than 2-hour incubation at both 4°C and 37°C (**Figure 6**). In consistent with other study²¹, macrophages incubated with 100 μM of nonencapsulated EGCG or NLCE at 4°C had higher EGCG content than those incubated at 37°C (**Figure 6**). The high stability of nonencapsulated EGCG and NLCE at 4°C may partially contribute to the results. Another reason might be an increase in EGCG efflux from macrophages at 37°C. Nonencapsulated EGCG at a concentration range from 5 to 640 μM is taken up by cells through passive diffusion process and subsequently converted to the methylated metabolites and glucuronides, which together with nonencapsulated EGCG may be pumped out by cells through multi-drug-resistance proteins or P-glycoproteins^{21,45}. This efflux rate was higher at 37°C than it at 4°C. This energy-dependent efflux process may further explain why cellular EGCG content was higher at 4°C than it at 37°C.

In vitro release study

The release behavior of nonencapsulated EGCG and NLCE was investigated using a dialysis method. Dynamic dialysis was chosen for separation of free EGCG from NLCE. In **Figure 7**, nonencapsulated EGCG exhibited a much faster dissolution rate with 100% released within the initial 2-hour period. In contrast, only 2% of EGCG was released from NLCE within the first 2 hours. After 9 hours, only 4.43% of EGCG was released from NLCE (**Figure 7**). The data indicated that increased cellular EGCG content by NLCE was due to uptake of nanocarriers, not nonencapsulated EGCG released from nanocarriers. We confirmed this result with the ultrafiltration method (Millipore Amicon Ultra-15). More

studies are required to investigate the membrane receptors in transporting NLCE and CSNLCE, organelles and enzymes for metabolizing them.

Cytotoxicity study

After treating THP-1 macrophages with 5, 10, and 20 μM of nonencapsulated or nanoencapsulated EGCG (NLCE and CSNLCE) and responsive void nanocarriers (VNLC and VCSNLC) for 18 hours, the cell viability was more than 90% among all treatments (**Figure 8**). The data indicate the NLCE and CSNLCE and their void nanocarriers had a very low level of toxicity in the tested concentration range.

Macrophage cholesterol accumulation

In the absence or presence of minimally oxLDL in the culture medium, nanoencapsulated EGCG significantly decreased macrophage CE content as compared to 1 X PBS, nonencapsulated EGCG and void nanocarriers. In the absence of oxLDL, CSNLCE and NLCE resulted in 9.4-fold and 2.7-fold lower macrophage CE content than nonencapsulated EGCG, respectively (**Figure 9A**). In the presence of minimally oxLDL, CSNLCE and NLCE resulted in 5.2-fold and 2.9-fold lower macrophage CE content than nonencapsulated EGCG, respectively (**Figure 9B**). Even though NLCE and CSNLCE decreased macrophage TC content, but they did not reach a statistical difference due to high standard deviations. The rate-limiting enzyme in cholesterol biosynthesis is 3-hydroxy-3-methyl-glutaryl-CoA reductase (HMGCR)¹⁰. Nonencapsulated EGCG at 50 μM or higher concentrations can decrease de novo cholesterol synthesis through decreasing HMGCR expression and activity^{10, 46}. Miura Y et al. fed male apolipoprotein E null mice with an atherogenic diet (high fat and cholesterol) in combination with a green tea extract drink (0.8 g/L), or a vehicle drink⁴⁷. The green tea extract drink decreased the atheromatous area and aortic cholesterol content by 23% and 27%, respectively⁴⁷. In the current study, NLCE and CSNLCE containing 10 μM of EGCG significantly decreased macrophage CE content, but nonencapsulated EGCG at the same concentration had no effect on lowering macrophage cholesterol content. The data indicate that nanoencapsulated EGCG retains its bioactivities and exhibits high efficacy at low dose.

Expression and secretion of inflammatory factors

As compared to nonencapsulated EGCG, NLCE significantly decreased mRNA levels of MCP-1 (**Figure 10A**), and CSNLCE significantly decreased MCP-1 release from macrophages (**Figure 10B**). The release of TNF α and IL-6 from macrophages and mRNA levels of TNF α was similar among all treatments (data not shown). MCP-1 promotes the recruitment of monocytes into the aortic intima layer and atherosclerotic lesion development⁷. Human studies have shown that elevated plasma MCP-1 concentrations can serve as a direct marker of atherosclerosis^{7, 48}. EGCG decreased mRNA and protein levels of MCP-1 in human endothelial cells in a dose-dependent manner (5-30 μM) through inhibiting p38 mitogen-activated protein kinases (MAPK) and nuclear factor-kappaB (NF- κB) activation¹¹. After treating monocytes or macrophages with 100 μM of EGCG, MCP-1 expression and secretion, and THP-1 migration were inhibited via inhibiting NF- κB activation^{12, 13}. When rodents were fed with a diet containing EGCG, blood MCP-1 concentrations were decreased^{49, 50}.

In summary, NLCE and CSNLCE significantly enhanced EGCG stability, improved its sustained release, increased its cellular bioavailability, decreased cholesterol content and MCP-1 expression in macrophages, which have a potential for preventing and reversing atherosclerotic lesion development.

Acknowledgments

The authors would like to thank Ming Sun for giving experimental help. The project described was supported by Grant Number R15AT007013 from the National Center For Complementary & Alternative Medicine. The content is solely the responsibility of the authors and does not necessarily represent the official views of the National Center For Complementary & Alternative Medicine or the National Institutes of Health.

ABBREVIATIONS USED

EGCG	(–)-epigallocatechin-3-gallate
NLCE	EGCG encapsulated chitosan-coated nanoliposomes
HPLC	high-performance liquid chromatography
MTT	3-(4,5-dimethylthiazol-2-yl)-2,5-diphenyltetrazolium bromide
SPSS	Statistical Package for the Social Sciences
ANOVA	One-way analysis of variance
SD	standard deviation
NLCs	nanostructured lipid carriers
NLCE	EGCG encapsulated nanostructured lipid carriers
CSNLCE	chitosan coated NLCE
VNLC	void NLC
VCSNLC	void CSNLC
PMA	phorbol 12- myristate 13-acetate
NBD-PC	7-nitro-2-1, 3-benzoxadiazol-4-yl-phosphatidylcholine
MCP-1	monocyte chemoattractant protein-1
CVD	cardiovascular disease
LDL	low density lipoprotein
oxLDL	oxidized LDL
1 X PBS	1 X phosphate buffered saline
SOD	superoxide dismutases
TEM	transmission electron microscope
FC	non-esterified/free cholesterol
TC	total cholesterol
CE	cholesteryl ester
TNF α	tumor necrosis factor alpha
IL-6	interleukin-6
PI	polydispersity index
HMGR	3-hydroxy-3-methyl-glutaryl-CoA reductase
MAPK	p38 mitogen-activated protein kinases
NF-κB	nuclear factor-kappaB

REFERENCES

1. Wang S, Noh SK, Koo SI. Green tea catechins inhibit pancreatic phospholipase A(2) and intestinal absorption of lipids in ovariectomized rats. *J Nutr Biochem*. 2006; 17(7):492–8. [PubMed: 16713229]
2. Basu A, Lucas EA. Mechanisms and effects of green tea on cardiovascular health. *Nutr Rev*. 2007; 65(8 Pt 1):361–75. [PubMed: 17867370]
3. Ananingsih VK, Sharma A, Zhou W. B Green tea catechins during food processing and storage: A review on stability and detection. *Food Research International*. 2013; 50:469–479.
4. Stangl V, Dreger H, Stangl K, Lorenz M. Molecular targets of tea polyphenols in the cardiovascular system. *Cardiovasc Res*. 2007; 73(2):348–58. [PubMed: 17020753]
5. Organization WH. The World Health Organization Report 2007- Cardiovascular Diseases. 2006
6. Go AS, Mozaffarian D, Roger VL, Benjamin EJ, Berry JD, Borden WB, Bravata DM, Dai S, Ford ES, Fox CS, Franco S, Fullerton HJ, Gillespie C, Hailpern SM, Heit JA, Howard VJ, Huffman MD, Kissela BM, Kittner SJ, Lackland DT, Lichtman JH, Lisabeth LD, Magid D, Marcus GM, Marelli A, Matchar DB, McGuire DK, Mohler ER, Moy CS, Mussolino ME, Nichol G, Paynter NP, Schreiner PJ, Sorlie PD, Stein J, Turan TN, Virani SS, Wong ND, Woo D, Turner MB. Heart disease and stroke statistics--2013 update: a report from the American Heart Association. *Circulation*. 2013; 127(1):e6–e245. [PubMed: 23239837]
7. Martinovic I, Abegunewardene N, Seul M, Vosseler M, Horstick G, Buerke M, Darius H, Lindemann S. Elevated monocyte chemoattractant protein-1 serum levels in patients at risk for coronary artery disease. *Circ J*. 2005; 69(12):1484–9. [PubMed: 16308496]
8. Ross R, Harker L. Hyperlipidemia and atherosclerosis. *Science*. 1976; 193(4258):1094–100. [PubMed: 822515]
9. Guyton JR, Klemp KF. Development of the lipid-rich core in human atherosclerosis. *Arterioscler Thromb Vasc Biol*. 1996; 16(1):4–11. [PubMed: 8548424]
10. Cuccioloni M, Mozzicafreddo M, Spina M, Tran CN, Falconi M, Eleuteri AM, Angeletti M. Epigallocatechin-3-gallate potently inhibits the in vitro activity of hydroxy-3-methyl-glutaryl-CoA reductase. *J Lipid Res*. 2011; 52(5):897–907. [PubMed: 21357570]
11. Hong MH, Kim MH, Chang HJ, Kim NH, Shin BA, Ahn BW, Jung YD. (–)-Epigallocatechin-3-gallate inhibits monocyte chemotactic protein-1 expression in endothelial cells via blocking NF-kappaB signaling. *Life Sci*. 2007; 80(21):1957–65. [PubMed: 17379255]
12. Joo SY, Song YA, Park YL, Myung E, Chung CY, Park KJ, Cho SB, Lee WS, Kim HS, Rew JS, Kim NS, Joo YE. Epigallocatechin-3-gallate Inhibits LPS-Induced NF-kappaB and MAPK Signaling Pathways in Bone Marrow-Derived Macrophages. *Gut Liver*. 2012; 6(2):188–96. [PubMed: 22570747]
13. Melgarejo E, Medina MA, Sanchez-Jimenez F, Urdiales JL. Epigallocatechin gallate reduces human monocyte mobility and adhesion in vitro. *Br J Pharmacol*. 2009; 158(7):1705–12. [PubMed: 19912233]
14. Chyu KY, Babbidge SM, Zhao X, Dandillaya R, Rietveld AG, Yano J, Dimayuga P, Cercek B, Shah PK. Differential effects of green tea-derived catechin on developing versus established atherosclerosis in apolipoprotein E-null mice. *Circulation*. 2004; 109(20):2448–53. [PubMed: 15136500]
15. Wolfram S. Effects of green tea and EGCG on cardiovascular and metabolic health. *J Am Coll Nutr*. 2007; 26(4):373S–388S. [PubMed: 17906191]
16. Arab L, Liu W, Elashoff D. Green and black tea consumption and risk of stroke: a meta-analysis. *Stroke*. 2009; 40(5):1786–92. [PubMed: 19228856]
17. Chen L, Lee MJ, Li H, Yang CS. Absorption, distribution, elimination of tea polyphenols in rats. *Drug Metab Dispos*. 1997; 25(9):1045–50. [PubMed: 9311619]
18. Warden BA, Smith LS, Beecher GR, Balentine DA, Clevidence BA. Catechins are bioavailable in men and women drinking black tea throughout the day. *J Nutr*. 2001; 131(6):1731–7. [PubMed: 11385060]
19. Lee MJ, Maliakal P, Chen L, Meng X, Bondoc FY, Prabhu S, Lambert G, Mohr S, Yang CS. Pharmacokinetics of tea catechins after ingestion of green tea and (–)-epigallocatechin-3-gallate

- by humans: formation of different metabolites and individual variability. *Cancer Epidemiol Biomarkers Prev.* 2002; 11(10 Pt 1):1025–32. [PubMed: 12376503]
20. Lambert JD, Yang CS. Mechanisms of cancer prevention by tea constituents. *J Nutr.* 2003; 133(10):3262S–3267S. [PubMed: 14519824]
 21. Hong J, Lu H, Meng X, Ryu JH, Hara Y, Yang CS. Stability, cellular uptake, biotransformation, and efflux of tea polyphenol (–)-epigallocatechin-3-gallate in HT-29 human colon adenocarcinoma cells. *Cancer Res.* 2002; 62(24):7241–6. [PubMed: 12499265]
 22. Lu H, Meng X, Yang CS. Enzymology of methylation of tea catechins and inhibition of catechol-O-methyltransferase by (–)-epigallocatechin gallate. *Drug Metab Dispos.* 2003; 31(5):572–9. [PubMed: 12695345]
 23. Vaidyanathan JB, Walle T. Glucuronidation and sulfation of the tea flavonoid (–)-epicatechin by the human and rat enzymes. *Drug Metab Dispos.* 2002; 30(8):897–903. [PubMed: 12124307]
 24. Zhang L, Gu FX, Chan JM, Wang AZ, Langer RS, Farokhzad OC. Nanoparticles in medicine: therapeutic applications and developments. *Clin Pharmacol Ther.* 2008; 83(5):761–9. [PubMed: 17957183]
 25. Puri A, Loomis K, Smith B, Lee JH, Yavlovich A, Heldman E, Blumenthal R. Lipid-based nanoparticles as pharmaceutical drug carriers: from concepts to clinic. *Crit Rev Ther Drug Carrier Syst.* 2009; 26(6):523–80. [PubMed: 20402623]
 26. Dube A, Nicolazzo JA, Larson I. Chitosan nanoparticles enhance the intestinal absorption of the green tea catechins (+)-catechin and (–)-epigallocatechin gallate. *Eur J Pharm Sci.* 2010; 41(2): 219–25. [PubMed: 20600878]
 27. Dube A, Nicolazzo JA, Larson I. Chitosan nanoparticles enhance the plasma exposure of (–)-epigallocatechin gallate in mice through an enhancement in intestinal stability. *Eur J Pharm Sci.* 2011; 44(3):422–6. [PubMed: 21925598]
 28. Heurtault B, Saulnier P, Pech B, Proust JE, Benoit JP. A novel phase inversion-based process for the preparation of lipid nanocarriers. *Pharm Res.* 2002; 19(6):875–80. [PubMed: 12134960]
 29. de Pace RC, Liu X, Sun M, Nie S, Zhang J, Cai Q, Gao W, Pan X, Fan Z, Wang S. Anticancer activities of (–)-epigallocatechin-3-gallate encapsulated nanoliposomes in MCF7 breast cancer cells. *J Liposome Res.* 2013; 23(3):187–96. [PubMed: 23600473]
 30. Wang S, Wu D, Lamon-Fava S, Matthan NR, Honda KL, Lichtenstein AH. In vitro fatty acid enrichment of macrophages alters inflammatory response and net cholesterol accumulation. *Br J Nutr.* 2009; 102(4):497–501. [PubMed: 19660150]
 31. Lam WH, Kazi A, Kuhn DJ, Chow LM, Chan AS, Dou QP, Chan TH. A potential prodrug for a green tea polyphenol proteasome inhibitor: evaluation of the peracetate ester of (–)-epigallocatechin gallate [(–)-EGCG]. *Bioorg Med Chem.* 2004; 12(21):5587–93. [PubMed: 15465336]
 32. Zhong Y, Chiou YS, Pan MH, Shahidi F. Anti-inflammatory activity of lipophilic epigallocatechin gallate (EGCG) derivatives in LPS-stimulated murine macrophages. *Food Chem.* 2012; 134(2): 742–8. [PubMed: 23107686]
 33. Barras A, Mezzetti A, Richard A, Lazzaroni S, Roux S, Melnyk P, Betbeder D, Monfilliet-Dupont N. Formulation and characterization of polyphenol-loaded lipid nanocapsules. *Int J Pharm.* 2009; 379(2):270–7. [PubMed: 19501139]
 34. Nishiyama N. Nanomedicine: nanocarriers shape up for long life. *Nat Nanotechnol.* 2007; 2(4): 203–4. [PubMed: 18654260]
 35. Dube A, Nicolazzo JA, Larson I. Chitosan nanoparticles enhance the intestinal absorption of the green tea catechins (+)-catechin and (–)-epigallocatechin gallate. *Eur J Pharm Sci.* 2010; 41(2): 219–25. [PubMed: 20600878]
 36. Dhawan S, Kapil R, Singh B. Formulation development and systematic optimization of solid lipid nanoparticles of quercetin for improved brain delivery. *J Pharm Pharmacol.* 2011; 63(3):342–51. [PubMed: 21749381]
 37. Iqbal MA, Md S, Sahni JK, Baboota S, Dang S, Ali J. Nanostructured lipid carriers system: recent advances in drug delivery. *J Drug Target.* 2012; 20(10):813–30. [PubMed: 22931500]
 38. Chen Z, Zhu QY, Tsang D, Huang Y. Degradation of green tea catechins in tea drinks. *J Agric Food Chem.* 2001; 49(1):477–82. [PubMed: 11170614]

39. Teeranachaideekul V, Muller RH, Junyaprasert VB. Encapsulation of ascorbyl palmitate in nanostructured lipid carriers (NLC)--effects of formulation parameters on physicochemical stability. *Int J Pharm*. 2007; 340(1-2):198–206. [PubMed: 17482778]
40. Wang R, Zhou W, Jiang X. Reaction kinetics of degradation and epimerization of epigallocatechin gallate (EGCG) in aqueous system over a wide temperature range. *J Agric Food Chem*. 2008; 56(8):2694–701. [PubMed: 18361498]
41. Dube A, Nicolazzo JA, Larson I. Chitosan nanoparticles enhance the plasma exposure of (–)-epigallocatechin gallate in mice through an enhancement in intestinal stability. *Eur J Pharm Sci*. 2011; 44(3):422–6. [PubMed: 21925598]
42. Sang S, Lee MJ, Hou Z, Ho CT, Yang CS. Stability of tea polyphenol (–)-epigallocatechin-3-gallate and formation of dimers and epimers under common experimental conditions. *J Agric Food Chem*. 2005; 53(24):9478–84. [PubMed: 16302765]
43. Long LH, Clement MV, Halliwell B. Artifacts in cell culture: rapid generation of hydrogen peroxide on addition of (–)-epigallocatechin, (–)-epigallocatechin gallate, (+)-catechin, and quercetin to commonly used cell culture media. *Biochem Biophys Res Commun*. 2000; 273(1):50–3. [PubMed: 10873562]
44. Yang GY, Liao J, Li C, Chung J, Yurkow EJ, Ho CT, Yang CS. Effect of black and green tea polyphenols on c-jun phosphorylation and H(2)O(2) production in transformed and non-transformed human bronchial cell lines: possible mechanisms of cell growth inhibition and apoptosis induction. *Carcinogenesis*. 2000; 21(11):2035–9. [PubMed: 11062165]
45. Borst P, Evers R, Kool M, Wijnholds J. A family of drug transporters: the multidrug resistance-associated proteins. *J Natl Cancer Inst*. 2000; 92(16):1295–302. [PubMed: 10944550]
46. Bursill CA, Roach PD. Modulation of cholesterol metabolism by the green tea polyphenol (–)-epigallocatechin gallate in cultured human liver (HepG2) cells. *J Agric Food Chem*. 2006; 54(5):1621–6. [PubMed: 16506810]
47. Miura Y, Chiba T, Tomita I, Koizumi H, Miura S, Umegaki K, Hara Y, Ikeda M, Tomita T. Tea catechins prevent the development of atherosclerosis in apolipoprotein E-deficient mice. *J Nutr*. 2001; 131(1):27–32. [PubMed: 11208934]
48. Deo R, Khera A, McGuire DK, Murphy SA, Meo Neto Jde P, Morrow DA, de Lemos JA. Association among plasma levels of monocyte chemoattractant protein-1, traditional cardiovascular risk factors, and subclinical atherosclerosis. *J Am Coll Cardiol*. 2004; 44(9):1812–8. [PubMed: 15519012]
49. Bose M, Lambert JD, Ju J, Reuhl KR, Shapses SA, Yang CS. The major green tea polyphenol, (–)-epigallocatechin-3-gallate, inhibits obesity, metabolic syndrome, and fatty liver disease in high-fat-fed mice. *J Nutr*. 2008; 138(9):1677–83. [PubMed: 18716169]
50. Senthil Kumaran V, Arulmathi K, Sundarapandian R, Kalaiselvi P. Attenuation of the inflammatory changes and lipid anomalies by epigallocatechin-3-gallate in hypercholesterolemic diet fed aged rats. *Exp Gerontol*. 2009; 44(12):745–51. [PubMed: 19732819]

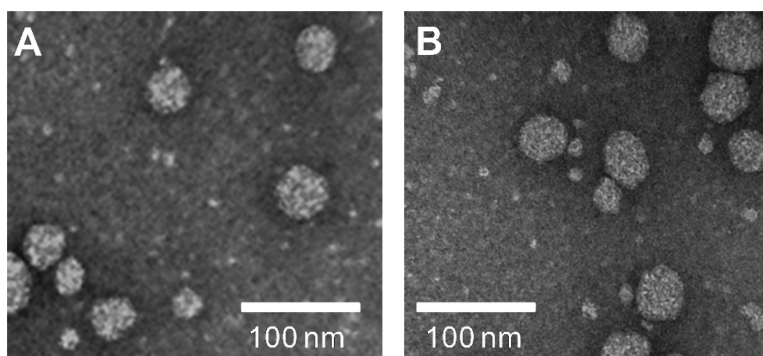


Figure 1. Transmission electron microscope (TEM) image of NLCE (**A**) and CSNLCE (**B**) stained by 2% of uranyl acetate.

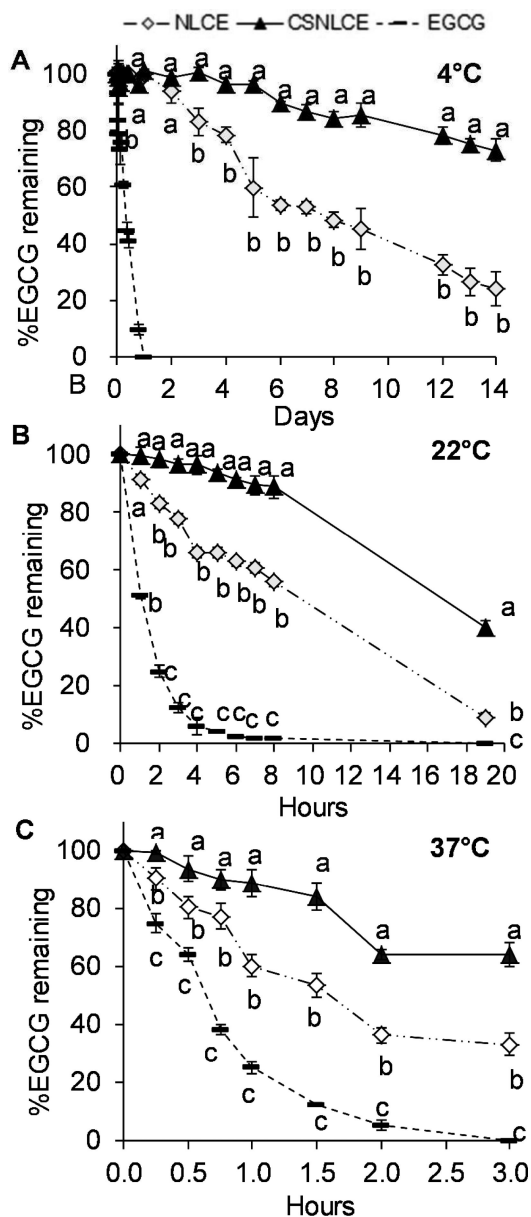


Figure 2. Stability of 100 μ M of nonencapsulated EGCG, NLCE and CSNLCE in 1 X PBS (pH 7.4) at 4°C (A), 22°C (B) and 37°C (C). Means at a time point without a common superscript differ, $P < 0.05$.

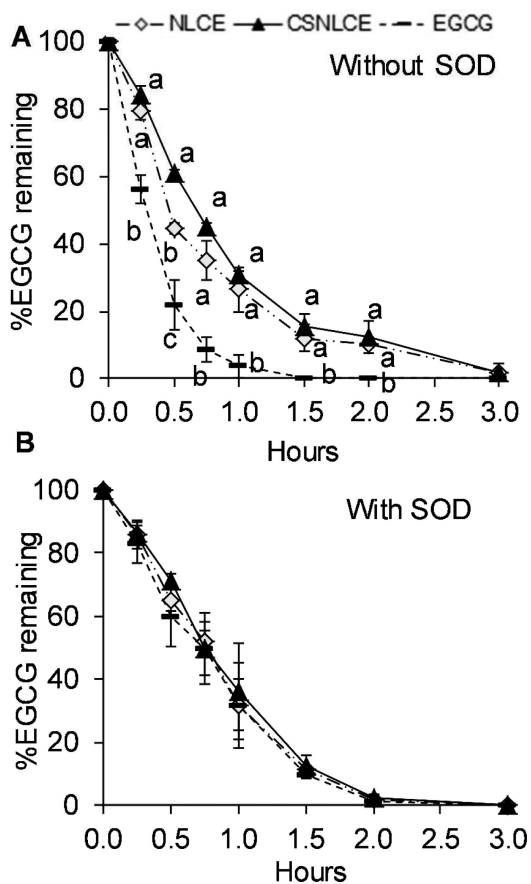


Figure 3. Stability of 100 μ M of nonencapsulated EGCG, NLCE and CSNLCE in RPMI1640 medium at 37°C in the absence of SOD (A); or in the presence of 5U/mL of SOD (B). Means at a time point without a common superscript differ, $P < 0.05$.

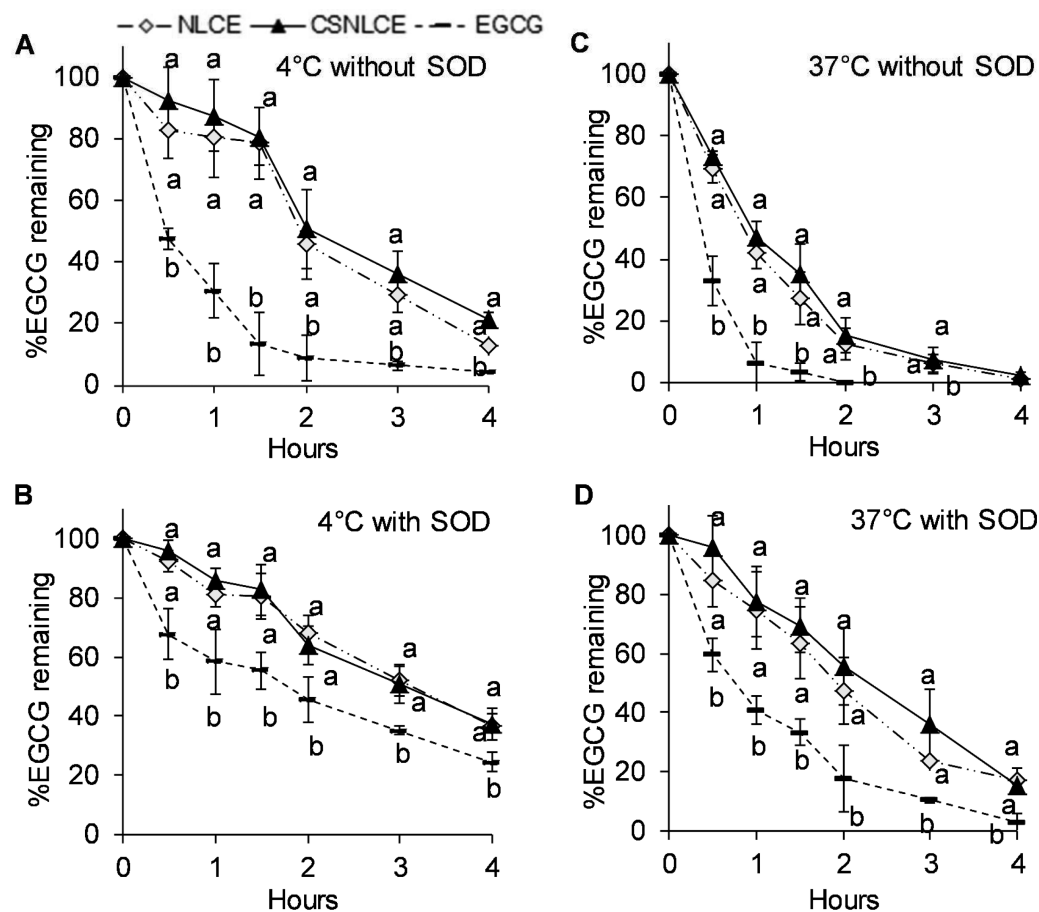
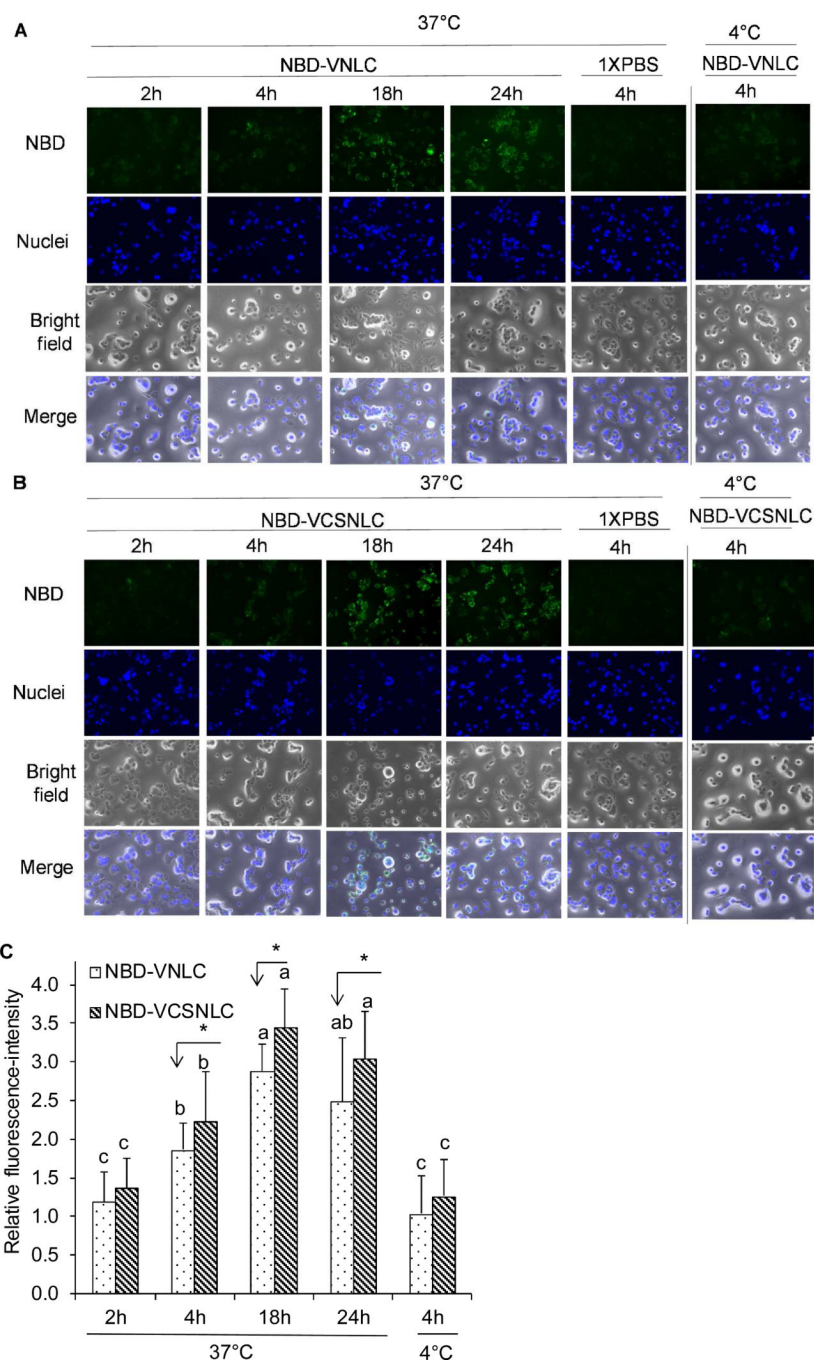


Figure 4.

Stability of 100 μ M of nonencapsulated EGCG, NLCE and CSNLCE in RPMI1640 medium in the presence of THP-1 derived macrophages at 4°C in the absence of SOD (A); at 4°C in the presence of 5U/mL of SOD (B); at 37°C in the absence of SOD (C); or at 37°C in the presence of 5U/mL of SOD (D). Means at a time point without a common superscript differ, $P < 0.05$.

**Figure 5.**

Representative fluorescence images of binding and uptake of NBD-VNLC (**A**) and NBD-VCSNLC (**B**) by THP-1 derived macrophages and quantification of relative fluorescence-intensities (**C**). Cells were incubated with NBD-VNLC and NBD-VCSNLC for 2, 4, 18, 24 hours at 37°C and 4 hours at 4°C. NBD emitted green fluorescence (λ of excitation is 460 nm, λ of emission is = 535 nm); cell nuclei were stained blue by DAPI (λ of excitation is 358 nm, λ of emission is 461 nm). The fluorescence-intensity of 1XPBS images was equal to 1. The fluorescence-intensities of other images were normalized by the intensity from 1XPBS. Compared to NBD-VNLC, NBD-VCSNLC had higher fluorescence-intensities at

37°C at hour 4, 18 and 24; *, $P < 0.05$; bars without a common superscript differ at different incubation time points and temperatures, $P < 0.05$.

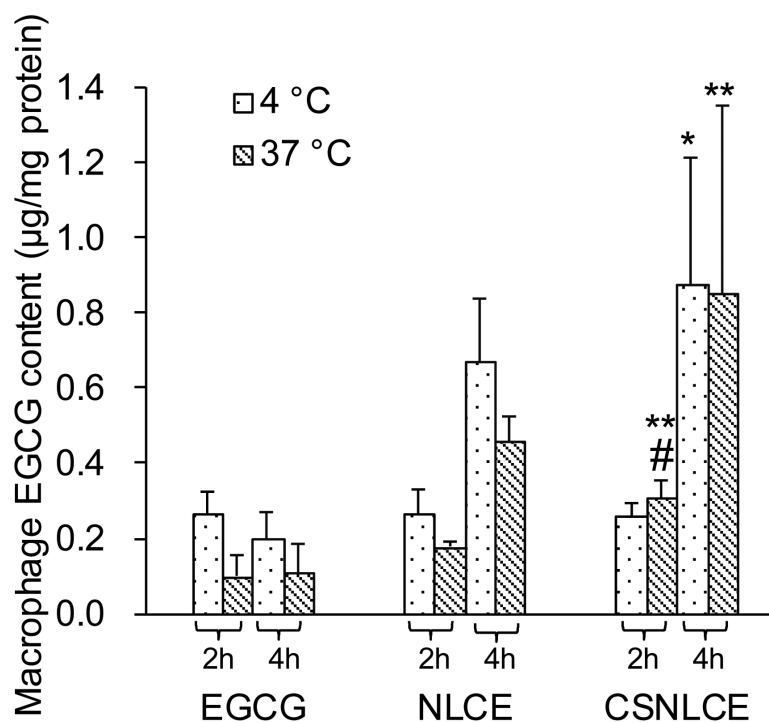


Figure 6.

Macrophage EGCG content. THP-1 derived macrophages were treated with 100 μM of nonencapsulated EGCG, NLCE, and CSNLCE in RPMI1640 medium containing SOD (5U/mL) for 2 and 4 hours at 4°C or 37°C. Three independent experiments were conducted. Compared to nonencapsulated EGCG, CSNLCE increased EGCG content *, $P < 0.05$; **, $p < P < 0.01$; compared to NLCE, CSNLCE increased EGCG content #, $P < 0.05$.

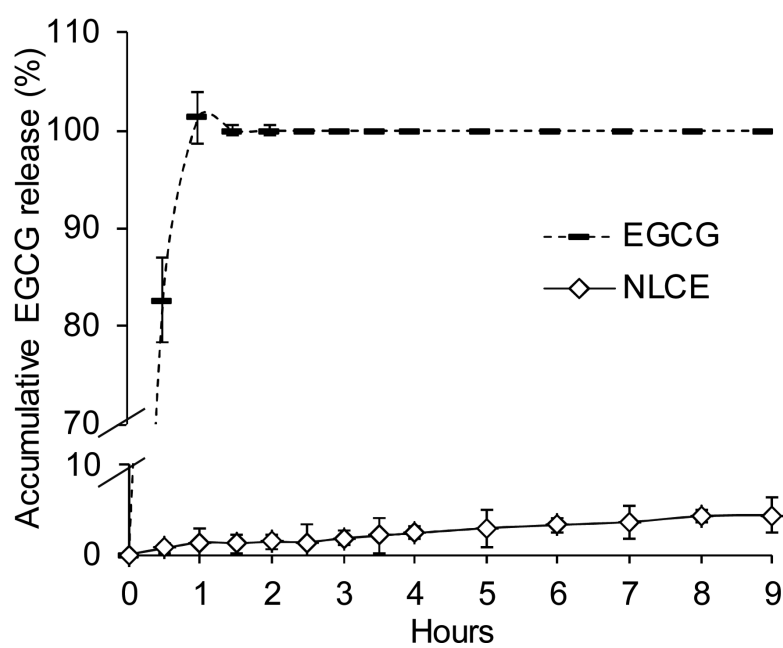


Figure 7.
In vitro EGCG release profiles of nonencapsulated EGCG and NLCE. Three independent experiments were conducted.

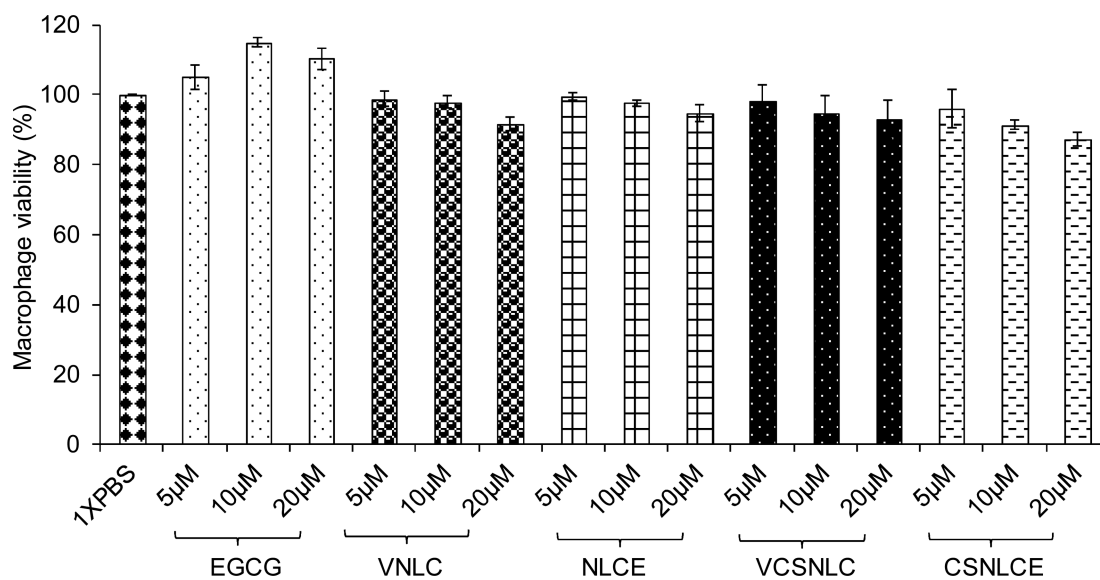


Figure 8.

Viability of THP-1 derived macrophages treated by 5, 10, and 20 μM of VNLC, VCSNLC, NLCE, CSNLCE, EGCG and 1 X PBS for 18 hours. Three independent experiments were conducted.

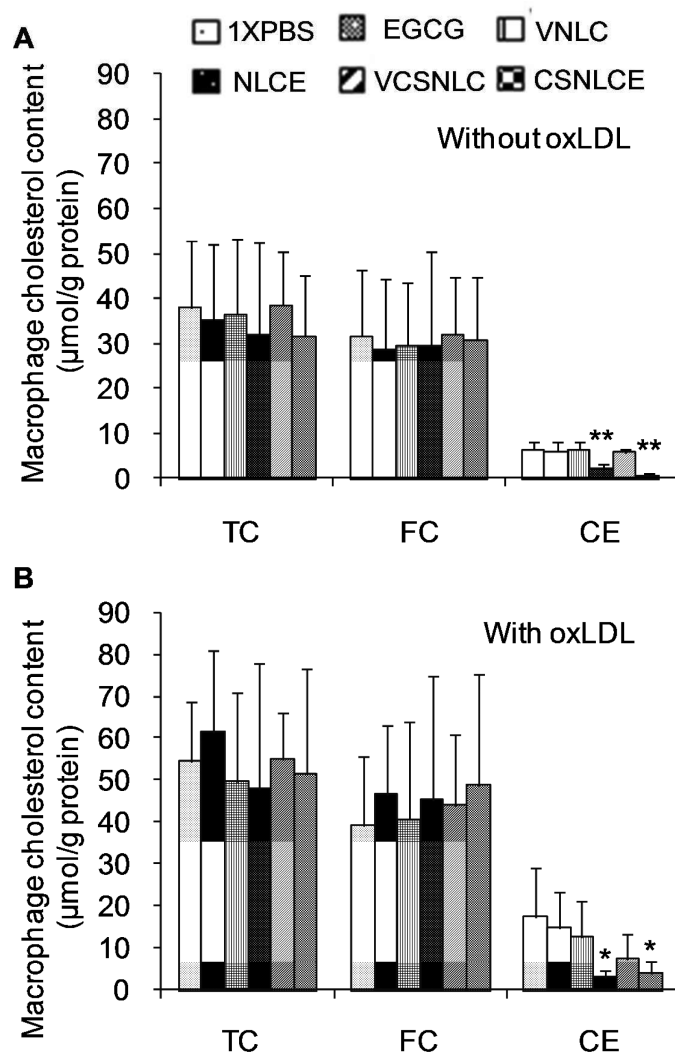


Figure 9.

Macrophage cholesterol content. THP-1 derived macrophages were treated with 10 μM of VNLC, VCSNLC, NLCE, CSNLCE, EGCG and 1 X PBS for 18 hours in the absence of minimally oxLDL (A), three independent experiments were conducted; and in the presence of oxLDL (B), six independent experiments were conducted. Compared to 1 X PBS, EGCG, VNLC and VCSNLC, NLCE and CSNLCE decreased macrophage CE content *, $P < 0.05$; **, $P < 0.01$.

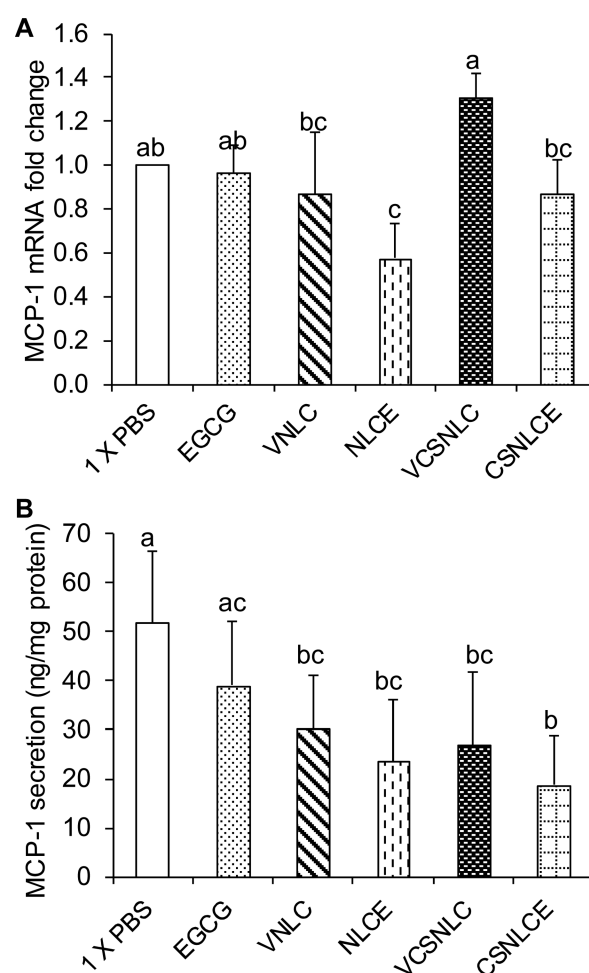


Figure 10. MCP-1 mRNA levels (**A**) and protein secretion (**B**) in/from THP-1 derived macrophages treated with 10 μ M of VNLC, VCSNLC, NLCE, CSNLCE, EGCG and 1 X PBS for 18 hours. Three independent experiments were conducted. Bars without a common superscript differ, $P < 0.05$.

Table 1

Particle size, zeta potential, polydispersity index (PI) of nanocarriers.

Nanocarriers		Particle size (nm)		Zeta potential (mV)		PI	
Temperature		0 day	50 days	0 day	50 days	0 day	50 days
4°C	VNLC	43.1±3.3	51.4±0.8	-8.9±3.0	-7.2±1.3	0.28±0.03	0.24±0.03
	NLCE	46.3±1.4	51.8±1.8	-12.6±3.2	-8.8±0.2	0.19±0.01	0.18±0.02
	VCSNLC	48.0±0.7	54.2±0.7	20.9±0.4	15.3±1.8	0.25±0.03	0.25±0.04
	CSNLCE	53.5±1.6	70.6±0.5	13.3±1.0	13.0±4.3	0.19±0.01	0.29±0.01
		0 hour	24 hours	0 hour	24 hours	0 hour	24 hours
37°C	VNLC	43.1±3.3	43.9±2.3	-8.9±3.0	-5.2±1.8	0.28±0.03	0.20±0.03
	NLCE	46.3±1.4	47.1±1.9	-12.6±3.2	-8.7±4.5	0.19±0.01	0.19±0.03
	VCSNLC	48.0±0.7	52.7±3.1	20.9±0.4	8.2±4.7	0.25±0.03	0.36±0.02
	CSNLCE	53.5±1.6	56.5±3.2	13.3±1.0	6.9±2.6	0.19±0.01	0.28±0.02